Available online at www.sciencedirect.com

jmr&t
Journal of Materials Research and Technology
www.jmrt.com.br

Original Article

Natural-synthetic fiber reinforced homogeneous and functionally graded vinylester composites: Effect of bagasse-Kevlar hybridization on wear behavior

Tej Singh[a], *Brijesh Gangil*[b,*], *Bharat Singh*[c], *Shashi Kant Verma*[d], *Don Biswas*[e], *Gusztáv Fekete*[a]

[a] *Savaria Institute of Technology, Eötvös Loránd University, Szombathely 9700, Hungary*
[b] *Mechanical Engineering Department, H.N.B. Garhwal University, 246174, India*
[c] *Mechanical Engineering Department, Phonics Group of Institutions, Roorkee 247667, India*
[d] *Mechanical Engineering Department, I.E.T. B.U. Jhansi, 284127, India*
[e] *University Science Instrumentation Centre, H.N.B. Garhwal University, 246174, India*

ARTICLE INFO

Article history:
Received 24 June 2019
Accepted 25 September 2019
Available online 31 October 2019

Keywords:
Bagasse fiber
Kevlar fiber
Graded composites
Sliding wear
Microscopy

ABSTRACT

In this work, vinylester resin based and hybrid Kevlar-bagasse fiber reinforced homogeneous and graded composites were developed and evaluated for wear performance on a pin-on-disc machine. An orthogonal array (L_{16}) was applied to examine the influence of four tribological control factors i.e. fiber content, normal load, sliding distance and sliding velocity. The experimental results indicate that normal load emerges as the most important factor affecting the wear rate of vinylester based graded and homogeneous composites with a contribution ratio of 36.33% and 32.09% respectively. Furthermore, composites worn surfaces were analyzed using scanning electron microscopy and the possible wear mechanism was studied.

1. Introduction

Present age can be considered as composite age with a lot of work being done on this field and still a vast number of new areas are being worked on [1–3]. Nowadays, the engineering composites are designed as to arrange the transition in micro/nano structures in order to improve the overall execution of the component [4–8]. Functionally graded materials (FGM) comes under the heading of these cutting edge composites where a gradient in morphology/microstructure is deliberately being made to suit a particular application and to enhance the performance levels superior to their homogeneous counterparts [9,10]. The early concept of FGM was proposed in Japan in 1984 [11]. Since then, researchers start exploring the area of FGM because of the multi-fold poten-

* *Corresponding author.*
E-mail: brijesh.gangil@hnbgu.ac.in (B. Gangil).
https://doi.org/10.1016/j.jmrt.2019.09.071

Table 1 – Physical and mechanical properties of the selected materials.

Property	Bagasse fiber	Kevlar fiber	Vinylester resin
Density (g/cm^3)	1.25	1.44	1.05
Tensile strength (MPa)	290	2600	80
Tensile modulus (GPa)	17	82	3
Elongation (%)	6.3	2.4	5

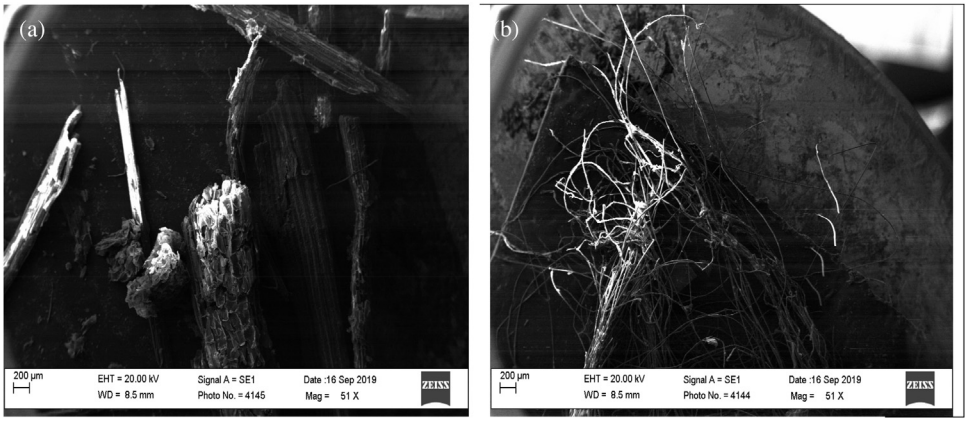

Fig. 1 – Scanning electron microscope images of (a) bagasse fiber and (b) Kevlar fiber.

tial of such materials in performance improvement. Since the last decade, material scientist had successfully developed various metal, ceramic and polymer based FGM to get the desired property gradient in the structure [12]. The functionally graded polymer composites having advantageous characteristics like high specific strength, high modulus, low weight, self-lubrication, low noise and ease in fabrication are a class of materials which is extensively used as components where friction and wear are critical issues [13,14]. Gangil et al. [15] studied the wear behaviour of fiber reinforced vinylester resin based FGM and homogeneous composites and found that FGM composites exhibit improved wear behaviour than homogeneous composites. Singh and Siddhartha [16] reported that the addition of glass fiber in polybutylene terephthalate graded composites contributed to escalated mechanical and thermo-mechanical properties in contrast with their homogeneous composites. Li et al. [17] successfully developed unidirectional continuous fiber reinforced polyethylene graded laminates and concluded that these graded composites exhibit 10–20% higher tensile strength compared to homogenous polyethylene composites. The influence of fiber hybridization (glass and carbon) on mechanical properties of graded epoxy composites was also investigated by Singh et al. [18]. They claimed that graded hybrid composite exhibits ~7-8% higher flexural modulus compared to classical hybrid composites.

Literature reveals that synthetic fibers such as glass, Kevlar, carbon and their combinations have been extensively used as reinforcement of polymeric graded composites. Generally, the synthetic fibers are incorporated with the main objective of improving the physico-mechanical and wear properties of the polymeric composites [19]. Apart from beneficial attributes these fibers are expansive, consumed higher energy, non-recyclable which may affect the final performance of the composite [20,21]. Recently, the increasing environmental awareness throughout the world has enforced the scientist to develop natural fiber reinforced polymer composites materials [22–25]. The natural fibers used in polymer composites offer various benefits such as environmental friendliness, light-weight, biodegradable, non-toxic, wide availability [26–29]. Despite the listed benefits, the natural fibers possess hydrophilic nature which leads to decline the physico-mechanical properties of the designed composites [30]. In this regard, hybridization of natural and synthetic fiber is reported to achieve higher performance properties, which would not be obtained with a single kind of reinforcement. Many studies have been conducted on the hybridization of natural-synthetic fiber such as bagasse-aramid by Anidha et al. [31], sugar palm-glass by Afzaluddin et al. [32], kenaf-glass by Ismail et al. [33] and curaua-aramid by Silva et al. [34] reported to improve the physico-mechanical, thermal and wear properties of the polymer composites.

Moreover one can expect that hybridization of synthetic fiber with natural fiber not only resulted in lower weight and cost with good physico-mechanical and wear properties but also reduces the environmental burden. However, there has been no systematic effort to evaluate the wear performance of an FGM containing synthetic and natural fibers in combination. Therefore, in current study, Kevlar and bagasse fibers reinforced vinylester based homogenous and graded composites were fabricated and evaluated for sliding wear performance.

2. Experimental details

2.1. *Materials and composite fabrication*

Vinylester resin, chopped bagasse and Kevlar fiber with an average size of 1–2 mm and 0.25 mm were taken as matrix

Table 2 – Detail of the composite composition and designation.

Composition (wt.%)	Designation								
	BK-0	BK-1	BK-2	BK-3	BK-4	BK-5	BK-6	BK-7	BK-8
Vinylester resin	100	95	90	85	80	95	90	85	80
Kevlar fiber	0	5	5	5	5	5	5	5	5
Bagasse fiber	0	0	5	10	15	0	5	10	15
Fabrication technique	Homogeneous					Graded			

Fig. 2 – Fabricated composites samples.

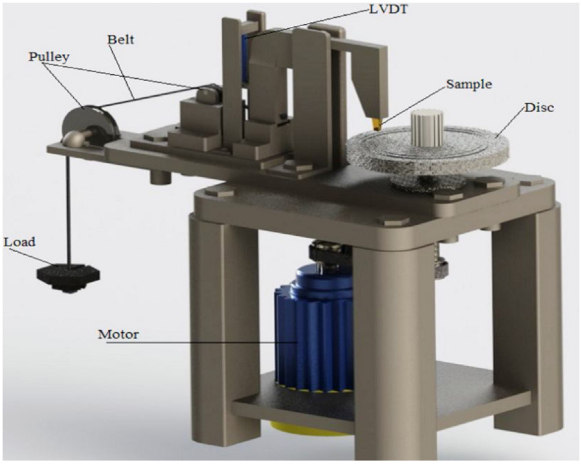

Fig. 3 – Scheme of pin-on-disc machine.

and reinforcing components. The ingredients were purchased from Dhanchan Industries Meerut, India. Chemically the bagasse fiber contains 37% cellulose, 22% lignin, 10% pectin and 21% hemicellulose [35]. The various properties of the selected ingredients are presented in Table 1, while the scanning electron microscope images of the selected bagasse and Kevlar fibers are presented in Fig. 1. Cobalt Naphthenate and ketone-peroxide in the ratio of 1.5:1 wt.% were used as accelerator and hardener. The fabrication of composite was initiated by mixing fiber in desired concentration with the resin, hardener and accelerator as presented in Table 2. Then after, the mixture was poured in glass tubes (Ø 10 mm, length = 110 mm). Gravity method is used for homogeneous composite, whereas vertical centrifugal casting technique is adopted for the fabrication of graded composites; where the known composition is taken in the glass tube and then rotated for 30 min at 1000 rpm. Then these specimens are kept further for curing at room temperature for 48 h and then taken out from the glass tube for wear tests. The developed composites are illustrated in Fig. 2.

2.2. *Sliding wear study*

The wear behaviour of the composites was analyzed as per ASTM G-99 test conditions. The wear tests were performed on a pin-on-disc machine (Fig. 3) equipped by DUCOM. The detailed schematic and working of the test rig is reported elsewhere [36]. A sequence of experiments were conducted with varying sliding velocities (1.5, 2.5, 3.5 and 4.5 m/s), normal load (10, 15, 20, 25 N), sliding distance (1, 2, 3, 4 km) and bagasse fiber loading (0, 5, 10, 15 wt.%) as given in Table 2. The material losses are measured by a precision electronic balance, while specific wear rate was determined as [37]:

$$\omega_s = \frac{\Delta w}{\partial \times t \times V_s \times \hbar_n} \quad (1)$$

Where, ω_s = specific wear rate (mm^3/Nm), Δw = sample weight loss (g), ∂ = density (g/mm^3), t = time (sec), V_s = sliding velocity (m/sec), $\hbar_n$ = applied load (N).

2.3. *Experiment design*

Taguchi method is a potent tool to analyze and optimize the impact of control factors on performance output. The Taguchi method contains following steps [38]:

Step I: Objective selection - The main characteristic of polymer composites is their wear performance. So, wear is selected as the main objective which has to be minimized.

Step II: Control factors and levels selection - Four control factors namely normal load, fiber loading, sliding speed and sliding distance with four levels each (Table 3) were utilized to study the wear behaviour of the composites.

Step III: Orthogonal array construction- The vital parts of the Taguchi method is the construction of orthogonal array. In the present work, an orthogonal array of L_{16} is taken as shown in Table 4.

Step IV: S/N ratio determination- In this step the obtained wear results were transformed into a signal to noise (S-N) ratio. Generally, higher-the-better, lower-the-better and nominal-

Table 3 – Levels of the control factor used in the experiment.

Controls factors	Levels				Units
	I	II	III	IV	
Sliding velocity (A)	1.5	2.5	3.5	4.5	m/s
Fiber content (B)	0	5	10	15	wt.%
Normal load (C)	10	15	20	25	N
Sliding distance (D)	1	2	3	4	km

Table 4 – Experimental design.

Test run	Control factors			
	A: Sliding velocity	B: Fiber content	C: Normal load	D: Sliding distance
1	1.5	0	10	1
2	1.5	5	15	2
3	1.5	10	20	3
4	1.5	15	25	4
5	2.5	0	15	3
6	2.5	5	10	4
7	2.5	10	25	1
8	2.5	15	20	2
9	3.5	0	20	4
10	3.5	5	25	3
11	3.5	10	10	2
12	3.5	15	15	1
13	4.5	0	25	2
14	4.5	5	20	1
15	4.5	10	15	4
16	4.5	15	10	3

the-better characteristics were used in the transformation. In current study, lower wear is desired hence, lower-the-better characteristics used for S-N ratio calculation [38]:

$$S-Nratio = -10\log\frac{1}{n}\left(\sum y^2\right) \quad (2)$$

Where y represents the W_s response and n denotes the number of experiments.

Step V: Contribution ratio (CR) determination- For effectiveness study, CR of each control factor was determined as [37]:

$$CR_i(\%) = \frac{(S-N)_{max,i} - (S-N)_{min,i}}{\sum_{i=1}^{j}\left[(S-N)_{max,i} - (S-N)_{min,i}\right]} \times 100 \quad (3)$$

Where, i = control factor, j = total number of control factors.

Step VI: Confirmation experiment- In the final step, a confirmation experiment is performed to validate the level of importance of the parameters taken during the analysis step.

3. Results and discussions

3.1. *Specific wear rate with respect to sliding velocity*

Plots of specific wear rate as a function of sliding velocity for neat vinylester and Kevlar-bagasse fiber based graded and homogeneous composites are illustrated in Fig. 4, while sliding distance (1 km) and normal load (10 N) remain fixed.

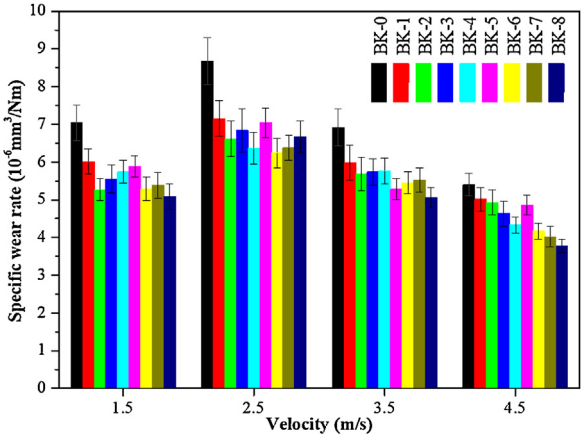

Fig. 4 – Specific wear rate as a function of sliding velocity.

The wear rate of the investigated composites (neat, homogeneous and graded) has been found to increase with rise in the sliding velocity to 2.5 m/s. Thereafter the wear rate decreased with further increase in sliding velocity from 2.5 to 4.5 m/s. The neat vinylester composite exhibits a higher wear rate to that of homogeneous and graded composites. The reduced wear for homogeneous and graded composites may be due to the self-lubricating nature and superior mechanical properties of the fibrous reinforcement [39]. From the graph, it is clear that, at higher sliding velocity, the graded composite with 15 wt.% bagasse fiber loading shows improved wear resistance as compared to the homogenous counterpart.

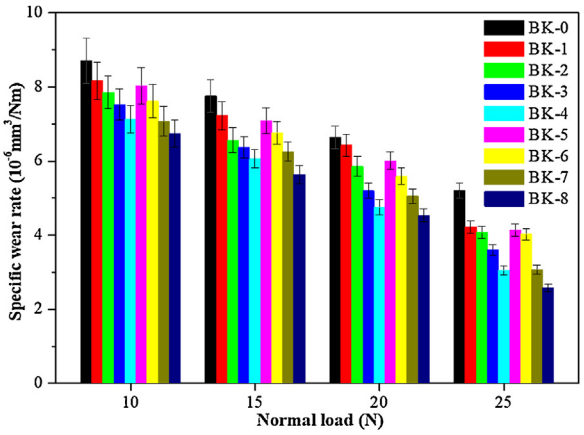

Fig. 5 – Specific wear rate as a function of normal load.

3.2. *Specific wear rate with respect to normal load*

Plots of specific wear rate as a function of normal load for neat vinylester and Kevlar-bagasse fiber based graded and homogeneous composites are illustrated in Fig. 5, while sliding distance (1 km) and sliding velocity (2.1 m/s) remain fixed.

As the load increases, the specific wear rate of graded/homogeneous composite decreases relative to the neat composite due to the more heat generation between the sliding surfaces. This may result in softening of the matrix and leads to the formation of a transfer film between two mating surfaces. This transfer film allows strong fiber-matrix bonding, which helps to reduce the interface de-bonding and also keeps the broken chopped fibers in the composite surface. This, in turn, prevents the early formation of third body abrasion [40]. Furthermore, due to the presence of Kevlar and bagasse fibers, the wear rate further decreases as they act as a blockade for the grooving and micro-ploughing mechanism of wear [41]. The graded composites show better wear resistance in contrast to their homogeneous counterpart for similar fiber loading and this is because better compaction and compatibility is achieved in case of graded composites due to centrifugal casting approach. Overall, 15 wt.% bagasse fiber reinforced graded composite exhibits a lower wear rate at higher velocity and load.

3.3. *Taguchi analysis of the composites*

Table 5 summarizes results of the Taguchi experimental design, presenting the specific wear rate of graded (W_{SG}) and homogeneous (W_{SH}) composites along with their respective S-N ratio. The overall means of the specific wear rate and the S-N ratio from all the experimental runs were $\sim 8.14 \times 10^{-6}$ mm^3/Nm and -18.10 dB for graded and $\sim 8.70 \times 10^{-6}$ mm^3/Nm and -18.66 dB for homogeneous composites respectively.

In addition, the lowest specific wear rate ($\sim 5.88 \times 10^{-6}$ mm^3/Nm) was found for test run 1 of graded composite and the highest specific wear rate ($\sim 12.34 \times 10^{-6}$ mm^3/Nm) for test run 13 of the homogeneous composite. Further, the S-N ratio response of wear rate for graded and homogeneous composites are provided in Table 6. From Table 6, one can easily infer that sliding velocity standout the most significant factor to influence the wear rate of the graded and homogeneous composites followed by fiber loading. However, the normal load and sliding distance are found to have less influence on the wear rate of the graded and homogeneous composites.

From Figs. 6 and 7, the optimum combination of control factors for the least wear rate of graded and homogeneous composites is determined as $A_1B_4C_1D_1$. The wear rates of homogeneous and graded composite material are shown in Table 5. From the test condition, it is obvious, that graded composite shows higher wear resistance than homogeneous composites. From this one can summarize that fabrication technique plays an important role in minimizing the wear. The contribution ratio of each control factor for wear rate of graded and homogeneous composites are determined and given in Fig. 8. The outcome demonstrates that normal load affects the wear rate of graded composites with a contribution ratio of 36.33% followed by fiber content, sliding velocity and sliding distance with a contribution ratio of 25.09%, 24.53% and 14.05% respectively. Normal load also has the strongest impact on the wear rate of homogeneous composites with a contribution ratio of 32.09% followed by sliding velocity, fiber content and sliding distance with a contribution ratio of 25%, 21.46% and 21.45%, respectively.

3.4. *Confirmation experiment*

For verifying the optimal condition for minimum specific wear rate obtained on the basis of Taguchi design, a confirmation test was conducted. The experiments were carried out under optimal conditions of control factors $A_1B_4C_1D_1$ to validate the reproducibility and feasibility of the Taguchi optimization. The predicted value of specific wear rate at optimal condition control factors i.e. $A_1B_4C_1D_1$ was calculated for graded and homogeneous composites using the following equations

$$\chi_G = \hbar + (A_1 - \hbar) + (B_4 - \hbar) + (C_1 - \hbar) + (D_1 - \hbar) \quad (4)$$

$$\chi_H = \lambda + (A_1 - \lambda) + (B_4 - \lambda) + (C_1 - \lambda) + (D_1 - \lambda) \quad (5)$$

Where, χ_G, $\hbar$ are the predicted average and overall experimental average of graded composite, χ_H, λ are the predicted average and overall experimental average of homogeneous composites respectively. The specific wear rate of graded composite by the predictive equation was found to be 5.40×10^{-6} mm^3/Nm and that for homogeneous composite is found to be 5.56×10^{-6} mm^3/Nm. The experimental results obtained are compared with the predicted results as shown in Table 7. An error of 2.96% and 3.42% for the specific wear rate has been observed for graded and homogeneous composites. This authenticates that the predicted values are reliable, consequently, Taguchi methodology can be said to be fit for predicting ideal control factors for wear minimization.

3.5. *Worn surface morphology*

For possible wear mechanism, the worn surfaces of the composites were investigated with the scanning electron microscope (SEM) and presented in Figs. 9–11. From SEM

Table 5 – Experimental results and corresponding S-N ratio.

Test run	W_{SG} 10^{-6} × (mm^3/Nm)	S-N ratio (db)	W_{SH} 10^{-6} × (mm^3/Nm)	S-N ratio (db)
1	5.880	−15.39	6.012	−15.58
2	6.716	−16.54	6.629	−16.43
3	8.260	−18.34	8.801	−18.89
4	8.605	−18.70	9.480	−19.54
5	10.18	−20.15	11.22	−21.00
6	8.370	−18.45	9.032	−19.12
7	7.512	−17.52	7.894	−17.95
8	7.026	−16.93	7.436	−17.43
9	8.602	−18.69	9.598	−19.64
10	8.684	−18.77	9.166	−19.24
11	8.354	−18.44	8.730	−18.82
12	8.211	−18.29	8.470	−18.56
13	11.40	−21.14	12.34	−21.83
14	9.076	−19.16	9.340	−19.41
15	7.046	−16.96	7.650	−17.67
16	6.365	−16.08	7.440	−17.43

Table 6 – S-N ratio response table for specific wear rate of graded and homogeneous composites.

	Level	Control factors			
		A	B	C	D
Average S-N ratio (dB) of graded composites	1	−17.24	−18.84	−17.09	−17.59
	2	−18.26	−18.23	−17.99	−18.26
	3	−18.55	−17.81	−18.28	−18.34
	4	−18.33	−17.50	−19.03	−18.20
Average S-N ratio (dB) of homogeneous composites	1	−17.61	−19.51	−17.74	−17.87
	2	−18.87	−18.55	−18.41	−18.63
	3	−19.07	−18.33	−18.84	−19.14
	4	−19.08	−18.24	−19.64	−18.99

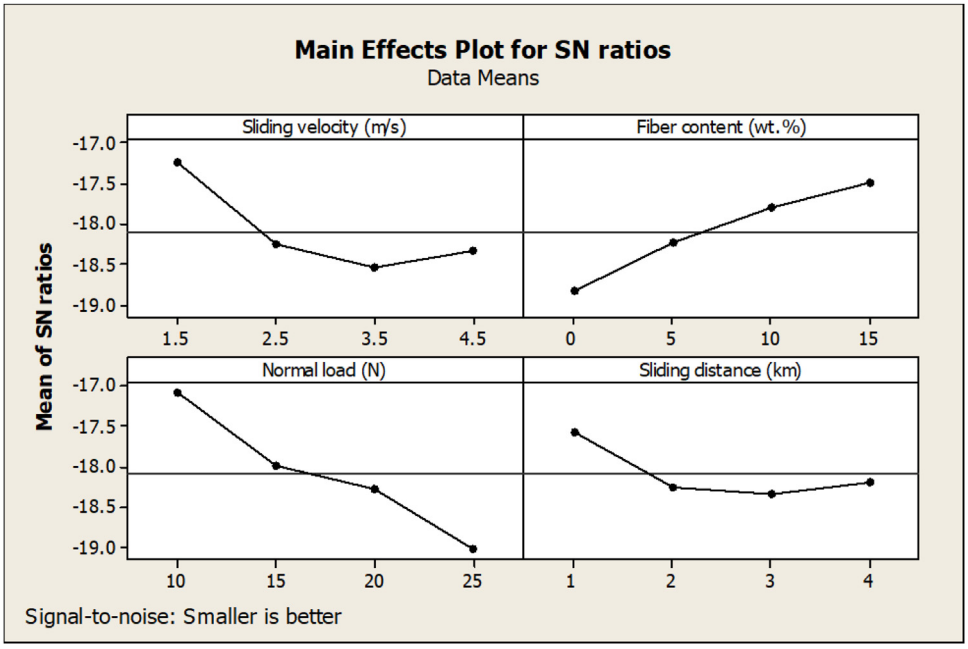

Fig. 6 – Main-effect plots for S-N ratio of specific wear rate of the graded composites.

observations it appears that composites (homogeneous or graded) under consideration exhibits various wear mechanism as per the operating conditions presented in Table 4. The wear behaviour of the composites varies with the fiber loading and operating conditions. The remarkable feature of the worn surfaces hybrid composites is a smooth topography. At lower sliding velocity, the worn surface was relatively smooth and wear rate increased with an increase

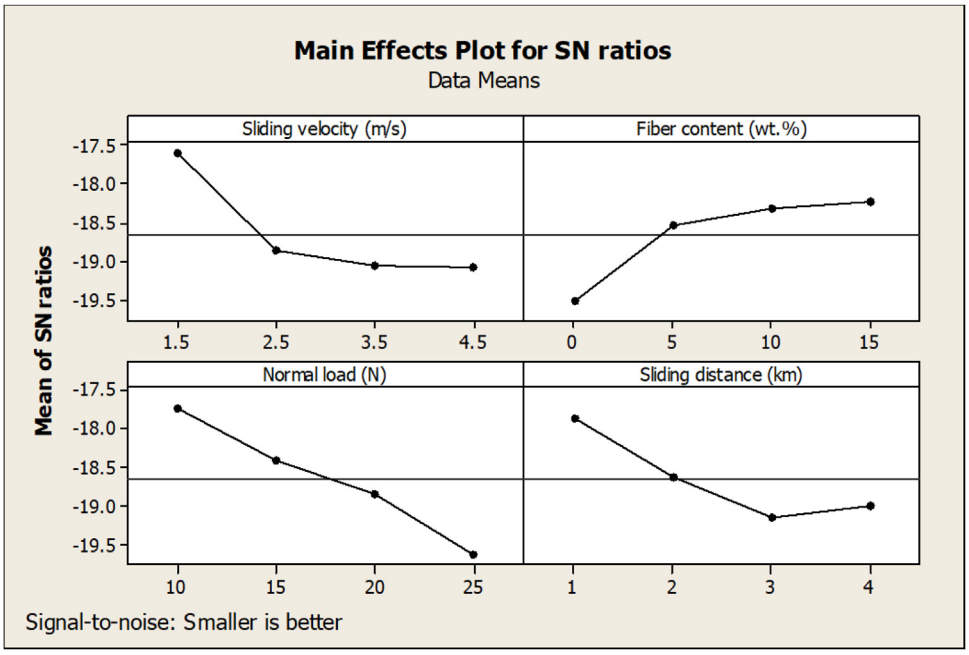

Fig. 7 – Main-effect plots for S-N ratio of specific wear rate of the homogeneous composites.

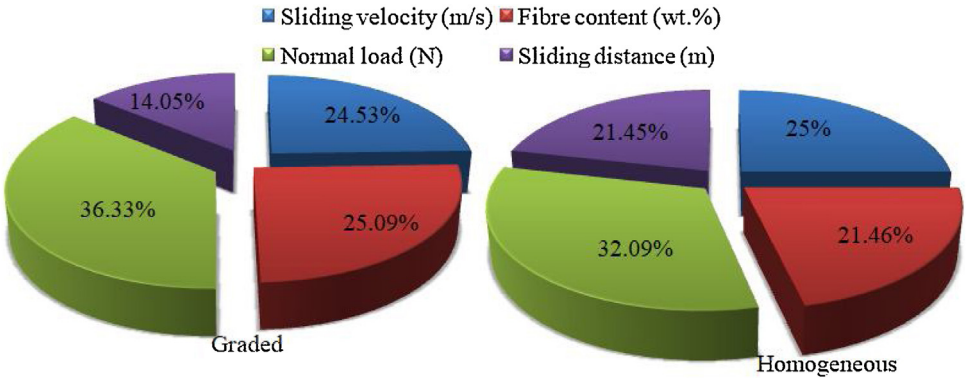

Fig. 8 – Contribution ratio of each control factor on specific wear rate of graded and homogeneous composites.

Table 7 – Outcomes of confirmation experiments.

	Optimum control factor		Error (%)
	Experimental	Predicted	
Graded	$A_1B_4C_1D_1$	$A_1B_4C_1D_1$	
Specific wear rate achieved $\times 10^{-6}$ mm^3/Nm	5.56	5.40	2.96
Homogeneous	$A_4B_1C_1D_1$	$A_4B_1C_1D_1$	
Specific wear rate achieved $\times 10^{-6}$ mm^3/Nm	5.75	5.56	3.42

in fiber loading and normal load. Fig. 9(a–d) of homogeneous and graded composite with ≤5 wt.% bagasse fiber loading, ≤15 N load, ≤2 km distance and 1.5 m/sec sliding velocity both exhibits almost similar wear rate which is in the range of ~5.88×10^{-6}–6.72×10^{-6} mm^3/Nm. This low wear rate of the composite at low sliding speed was due to this synergistic effect of bagasse and Kevlar fibers. Both homogeneous and graded composites show increased wear rate 9.48×10^{-6} mm^3/Nm and 8.61×10^{-6} mm^3/Nm respectively, As the bagasse fiber loading increases to 15 wt.%, normal load to 25 N, sliding distance to 4 km, as shown in Fig. 9(e, f).

In comparison with Fig. 9(a–d), it is clear that the worn surface of Fig. 9(e, f) for both homogeneous and graded composites exhibit higher wear rates with severe fiber breakage and surface damage. This severe fiber breakage and surface damage are due to frictional heat generated during sliding will leading to fiber-matrix debonding and hence increased wear rate [42]. The wear rate increased in both the

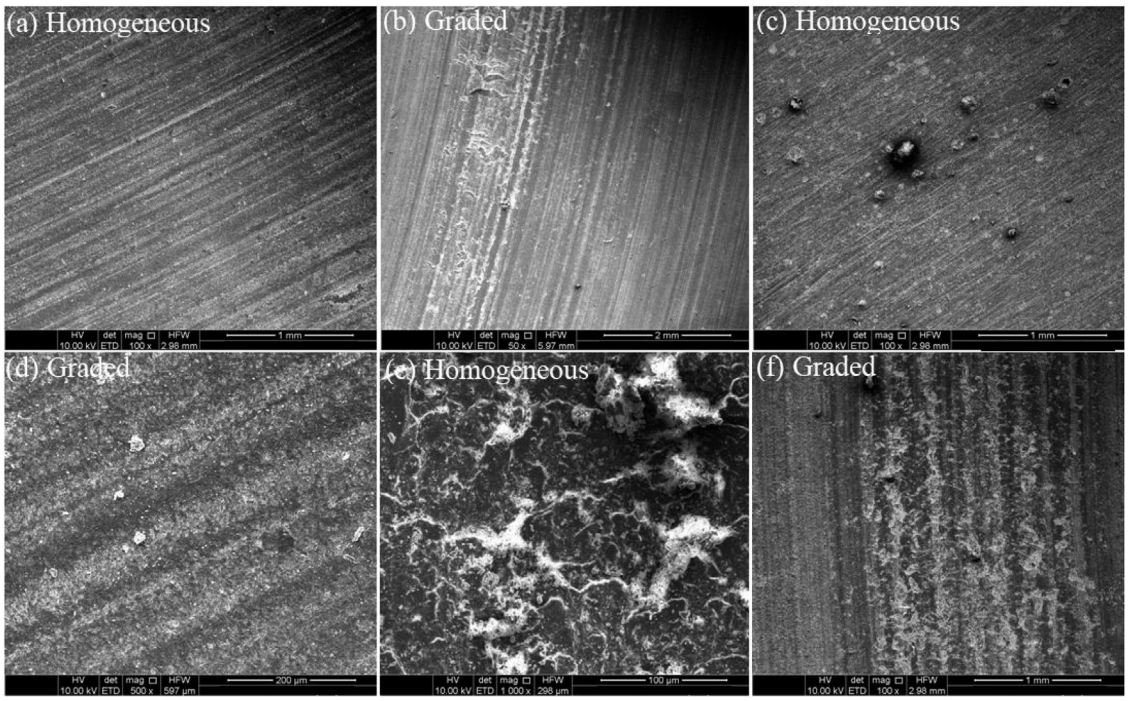

Fig. 9 – Worn surface morphology of homogeneous and graded composites.

graded and homogeneous composites and remain in the range of 8.37×10^{-6}–11.22×10^{-6} mm^3/Nm, as the sliding velocity increases to 2.5 m/s and sliding distance to 3–4 km (Table 4, Test run: 5–6). Their corresponding micrographs are shown in Fig. 10(a–d) reveals extensive matrix fragmentation and the manifestation of shallow furrows due to micro-ploughing in

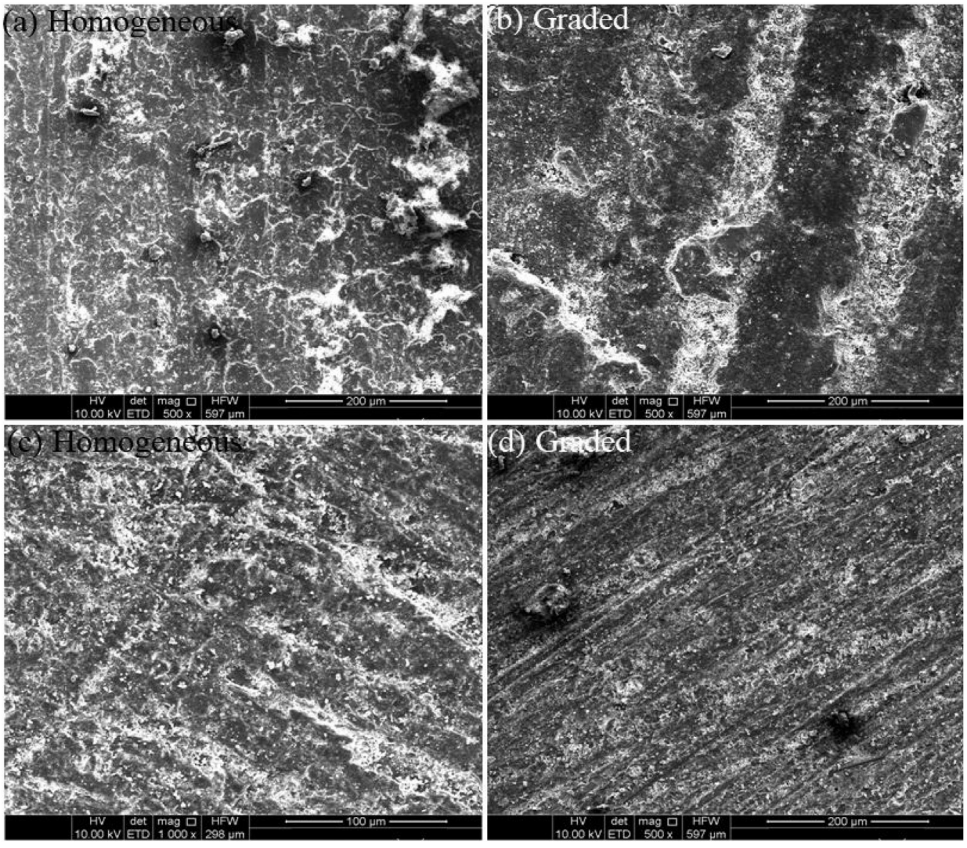

Fig. 10 – Worn surface morphology of homogeneous and graded composites.

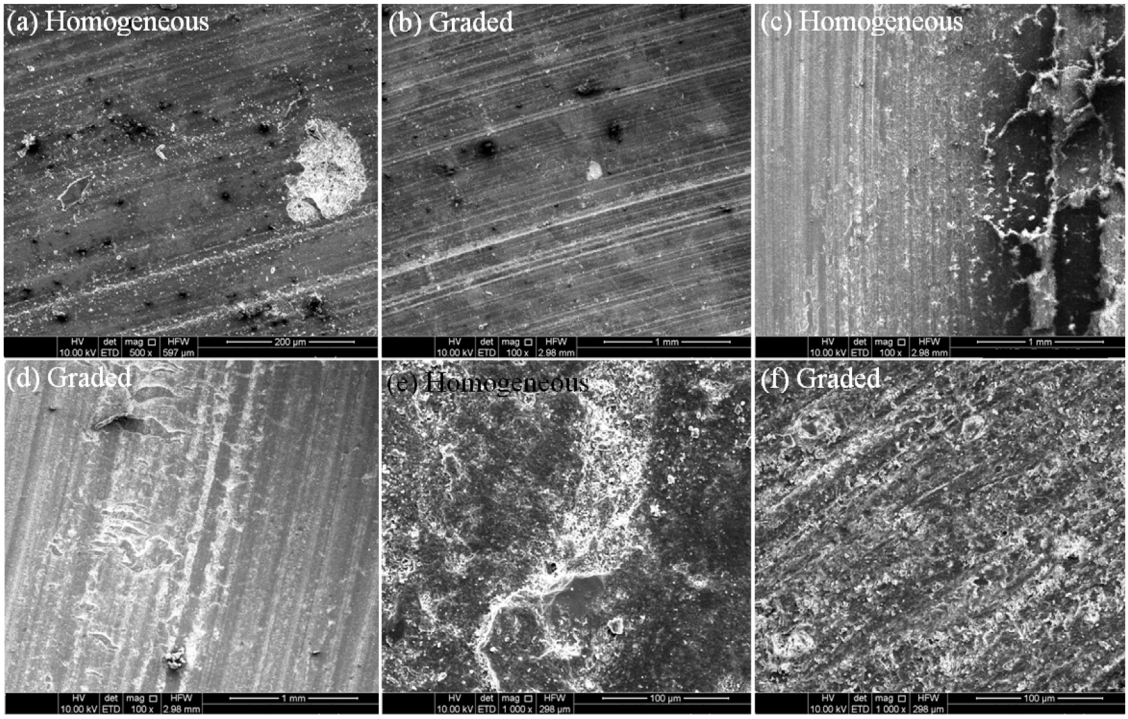

Fig. 11 – Worn surface morphology of homogeneous and graded composites.

the resin and micro-cutting of the fibers in both homogeneous and graded composites. This might be credited to the reduction of fiber-matrix adhesion with increased frictional heat resulted in higher wear rate due to peeling-off and pulverization of the fibers [43].

Fig. 11(a–d) shows the worn surface of ≤ 5 wt.% bagasse fiber reinforced composites tested under 20–25 N loads at 3.5 m/s of sliding speed and sliding distance of 3–4 km. The worn surfaces exhibit ploughed shear mark on the rubbing surface and fiber breakage and matrix wear debris accumulation of homogeneous and graded composites as shown in Fig. 11(a–d), (Table 4, Test run: 9–10) accounts for higher wear rate i.e. $\sim 9 \times 10^{-6}$ mm^3/N-m for both homogeneous and graded composites. Further, with an increase in sliding velocity to 4.5 m/s, bagasse fiber loading ≤ 5 wt.% and loads (≥20 N) wear rate increases tremendously for both homogeneous and graded composites and remains in between 9.076×10^{-6} and 12.34×10^{-6} mm^3/Nm. The distinct feature of the worn surface is the higher extent of fibers breakage or pulverization and debonding in the fiber-matrix adhesion. This may be attributed to the formation of large rough patches that appears on the worn surface as shown in Fig. 11(e, f). The protruding of fibers from shallow furrows drawn across the surface as a result of microploughing and extensive fibrillation of the fiber can also be seen. Also, delamination and thermo-fatigue failure of the matter from the surface of the composite is responsible for the highest wear rate.

4. Conclusions

In the present study, fixed Kevlar fiber (5 wt.%) and varying bagasse fiber (0, 5, 10, 15 wt.%) reinforced homogeneous and graded vinylester composites were designed, fabricated and evaluated for sliding wear behaviour. The specific wear rate of graded and homogeneous composites was first increased and then decreased with further increase in sliding velocity. Whereas, the specific wear rate shows a decreasing trend with an increased normal load. The minimum specific wear rate is shown by 15 wt.% bagasse fiber reinforced graded composite. The optimum combination of control factors to achieve minimum specific wear rate for homogeneous and graded composites is: 1.5 m/s sliding velocity (Factor A, Level 1), 15 wt.% bagasse fiber content (Factor B, Level 4), 10 N normal load (Factor C, Level 1) and 1 km sliding distance (Factor D, Level 1). The contribution of the normal load was the largest influence on the specific wear rate of graded and homogeneous composites with 36.33% and 32.09% respectively.

Conflict of interest

"The authors declare that they have no known competing financial interests or personal relationships that could have appeared to influence the work reported in this paper."

REFERENCES

[1] Ahmadian-Fard-Fini S, Ghanbari D, Salavati-Niasari M. Photoluminescence carbon dot as a sensor for detecting of *Pseudomonas aeruginosa* bacteria: hydrothermal synthesis of magnetic hollow $NiFe_2O_4$-carbon dots nanocomposite material. Composite B: Eng 2019;161:564–77.

[2] Ghanbari D, Salavati-Niasari M. Synthesis of urchin-like CdS-Fe_3O_4 nanocomposite and its application in flame

retardancy of magnetic cellulose acetate. J Ind Eng Chem 2015;24:284–92.
[3] Safajou H, Khojasteh H, Salavati-Niasari M, Mortazavi-Derazkola S. Enhanced photocatalytic degradation of dyes over graphene/Pd/TiO_2 nanocomposites: TiO_2 nanowires versus TiO_2 nanoparticles. J Colloid Interface Sci 2017;498:423–32.
[4] Ghanbari D, Salavati-Niasari M, Esmaeili-Zare M, Jamshidi P, Akhtarianfar F. Hydrothermal synthesis of CuS nanostructures and their application on preparation of ABS-based nanocomposite. J Ind Eng Chem 2014;20(5):3709–13.
[5] Jamshidi P, Ghanbari D, Salavati-Niasari M. Photocatalyst Al_2O_3-TiO_2: preparation of poly vinyl alcohol based nanocomposite by ultrasonic waves. J Mater Sci Mater Electron 2017;28(12):8950–9.
[6] Salavati-Niasari M, Davar F, Loghman-Estarki MR. Long chain polymer assisted synthesis of flower-like cadmium sulfide nanorods via hydrothermal process. J Alloys Compd 2009;481(1-2):776–80.
[7] Jamshidi P, Ghanbari D, Salavati-Niasari M. Sonochemical synthesis of $La(OH)_3$ nanoparticle and its influence on the flame retardancy of cellulose acetate nanocomposite. J Ind Eng Chem 2014;20(5):3507–12.
[8] Mahdiani M, Soofivand F, Ansari F, Salavati-Niasari M. Grafting of $CuFe_{12}O_{19}$ nanoparticles on CNT and graphene: Eco-friendly synthesis, characterization and photocatalytic activity. J Clean Prod 2018;176:1185–97.
[9] Sola A, Bellucci D, Cannillo V. Functionally graded materials for orthopedic applications - an update on design and manufacturing. Biotechnol Adv 2016;34:504–31.
[10] Oshkour AA, Pramanik S, Mehrali M, Yau YH, Tarlochan F, Osman NAA. Mechanical and physical behavior of newly developed functionally graded materials and composites of stainless steel 316L with calcium silicate and hydroxyapatite. J Mech Behav Biomed Mater 2015;49:321–31.
[11] Koizumi M, Niino M. Overview of FGM research in Japan. MRS Bull 1995;20:19–21.
[12] Udupa G, Rao SS, Gangadharan KV. Functionally graded composite materials: an overview. Procedia Mater Sci 2014;5:1291–9.
[13] Naebe M, Shirvanimoghaddam K. Functionally graded materials: a review of fabrication and properties. Appl Mater Today 2016;5:223–45.
[14] Almasi D, Sadeghi M, Lau WJ, Roozbahani F, Iqbal N. Functionally graded polymeric materials: a brif review of current fabrication methods and introduction of a novel fabrication method. Mater Sci Eng C 2016;64:102–7.
[15] Gangil B, Patnaik A, Kumar A, Kumar M. Investigations on mechanical and sliding wear behaviour of short fibre-reinforced vinylester-based homogenous and their functionally graded composites. Proc Inst Mech Eng Part L J Mater Des Appl 2012;226:300–15.
[16] Singh AK, Siddhartha. Mechanical and thermo-mechanical peculiarity of functionally graded materials-based glass fiber-filled polybutylene terephthalate composites. J Reinf Plast Compos 2018;37:410–26.
[17] Li L, Liu X, Zhou X, Hong J, Zhuang X, Yan X. Mechanical properties of unidirectional continuous fiber self-reinforced polyethylene graded laminates. Polym Compos 2015;36:128–37.
[18] Singh SB, Chawla H, Ranjitha B. Hybrid effect of functionally graded hybrid composites of glass-carbon fibers. Mech Adv Mater Struct 2019;26(14):1195–208.
[19] Liu Y, Ma Y, Lv X, Yu J, Zhuang J, Tong J. Mineral fibre reinforced friction composites: effect of rockwool fibre on mechanical and tribological behaviour. Mater Res Express 2018;5(9):095308.
[20] Reddy GR, Kumar MA, Karthikeyan N, Basha SM. Tamarind fruit fiber and glass fiber reinforced polyester composites. Mech Adv Mater Struct 2015;22:770–5.
[21] Singh T, Gangil B, Patnaik A, Biswas D, Fekete G. Agriculture waste reinforced cornstarch-based biocomposites: effect of rice husk/walnut shell on physicomechanical, biodegradable and thermal properties. Mater Res Express 2019;6(4):045702.
[22] Hamidon MH, Sultan MTH, Ariffin AH, Shah AUM. Effects of fibre treatment on mechanical properties of kenaf fibre reinforced composites: a review. J Mater Res Technol 2019;8(3):3327–37.
[23] Liu Y, Xie J, Wu N, Wang L, Ma Y, Tong J. Influence of silane treatment on the mechanical, tribological and morphological properties of corn stalk fiber reinforced polymer composites. Tribol Int 2019;131:398–405.
[24] Singh T, Tejyan S, Patnaik A, Singh V, Zsoldos I, Fekete G. Fabrication of waste bagasse fibre reinforced epoxy composites: study of physical, mechanical and erosion properties. Polym Compos 2019;40(9):3777–86.
[25] Fidelis MEA, Pereira TVC, Gomes OFM, Silva FA, Filho RDT. The effect of fiber morphology on the tensile strength of natural fibers. J Mater Res Technol 2013;2(2):149–57.
[26] Glória GO, Teles MCA, Neves ACC, Vieira CMF, Lopes FPD, Gomes MA, et al. Bending test in epoxy composites reinforced with continuous and aligned PALF fibers. J Mater Res Technol 2017;6(4):411–6.
[27] Singh T, Gangil B, Patnaik A, Kumar S, Rishiraj A, Fekete G. Physico-mechanical, thermal and dynamic mechanical behaviour of natural-synthetic fiber reinforced vinylester based homogenous and functionally graded composites. Mater Res Express 2019;6:025704.
[28] Liu Y, Wang L, Liu D, Ma Y, Tian Y, Tong J, et al. Evaluation of wear resistance of corn stalk fiber reinforced brake friction materials prepared by wet granulation. Wear 2019;432-433:102918.
[29] Oliveira CG, Margem FM, Monteiro SN, Lopes FPD. Comparison between tensile behavior of epoxy and polyester matrix composites reinforced with eucalyptus fibers. J Mater Res Technol 2017;6(4):406–10.
[30] Nascimento LFC, Monteiro SN, Louro LHL, Luz FS, Santos JL, Braga FO, et al. Charpy impact test of epoxy composites reinforced with untreated and mercerized mallow fibers. J Mater Res Technol 2018;7(4):520–7.
[31] Anidha S, Latha N, Muthukkumar M. Reinforcement of Aramid fiber with bagasse epoxy bio-degradable composite: investigations on mechanical properties and surface morphology. J Mater Res Technol 2019;8(3):3198–212.
[32] Afzaluddin A, Jawaid M, Salit MS, RidwanIshak M. Physical and mechanical properties of sugar palm/glass fiber reinforced thermoplastic polyurethane hybrid composites. J Mater Res Technol 2019;8(1):950–9.
[33] Ismail MF, Sultan MTH, Hamdan A, Shah AUM, Jawaid M. Low velocity impact behaviour and post-impact characteristics of kenaf/glass hybrid composites with various weight ratios. J Mater Res Technol 2019;8(3):2662–73.
[34] Silva AO, Monsores KGC, Oliveira SSA, Weber RP, Monteiro SN. Ballistic behavior of a hybrid composite reinforced with curaua and aramid fabric subjected to ultraviolet radiation. J Mater Res Technol 2018;7(4):584–91.
[35] Ramesh M, Palanikumar K, Reddy KH. Plant fibre based bio-composites: sustainable and renewable green materials. Renewable Sustainable Energy Rev 2017;79:558–84.
[36] Singh T, Chauhan R, Patnaik A, Gangil B, Nain R, Kumar A. Parametric study and optimization of multiwalled carbon nanotube filled friction composite materials using Taguchi method. Polym Compos 2018;39:E1109–17.
[37] Singh T, Patnaik A, Chauhan R, Chauhan P, Kumar N. Physico-mechanical and tribological properties of nanoclay

filled friction composite materials using Taguchi design of experiment approach. Polym Compos 2018;39:1575–81.
[38] Tejyan S, Singh T, Patnaik A, Fekete G, Gangil B. Physico-mechanical and erosive wear analysis of polyester fibre-based nonwoven fabric-reinforced polymer composites. J Ind Text 2019;49(4):447–64.
[39] Suresha B, Kumar KS, Seetharamu S, Kumaran PS. Friction and dry sliding wear behavior of carbon and glass fabric reinforced vinyl ester composites. Tribol Int 2010;43:602–9.
[40] Friedrich K, Liu Z, Hager AM. Recent advances in polymer composites' tribology. Wear 1995;190:139–44.
[41] Gong G, Yang H, Fu X. Tribological properties of kaolin filled UHMWPE composites in unlubricated sliding. Wear 2004;256:88–94.
[42] Zhao Q, Bahadur S. Investigation of the transition state in the wear of polyphenylene sulfide sliding against steel. Tribol Lett 2002;12:23–33.
[43] Basavarajappa S, Ellangovan S, Arun KV. Studies on dry sliding wear behaviour of graphite filled glass-epoxy composites. Mater Des 2009;30:2670–5.